Phosphodiesterase-8A binds to and regulates Raf-1 kinase

Kim M. Brown[a], Jon P. Day[a], Elaine Huston[a], Bastian Zimmermann[b], Kornelia Hampel[b], Frank Christian[a], David Romano[c], Selim Terhzaz[d], Louisa C. Y. Lee[a], Miranda J. Willis[a], David B. Morton[e], Joseph A. Beavo[f,1], Masami Shimizu-Albergine[f], Shireen A. Davies[d], Walter Kolch[c,g], Miles D. Houslay[h], and George S. Baillie[a]

[a]Institute of Cardiovascular and Medical Science and [d]Institute of Molecular, Cellular and Systems Biology, College of Medical, Veterinary and Life Sciences, University of Glasgow, Glasgow G12 8QQ, Scotland, United Kingdom; [b]Biaffin GmbH and Co KG, 34132 Kassel, Germany; [c]Systems Biology Ireland and [g]Conway Institute of Biomolecular and Biomedical Research, University College Dublin, Dublin 4, Ireland; [e]Department of Integrative Biosciences, Oregon Health Science University, Portland, OR 97239; [f]Department of Pharmacology, University of Washington, Seattle, WA 98159; and [h]Institute of Pharmaceutical Sciences, King's College London, London SE1 9NH, United Kingdom

Contributed by Joseph A. Beavo, February 20, 2013 (sent for review September 24, 2012)

V-raf-1 murine leukemia viral oncogene homolog 1 (Raf-1) is a key activator of the ERK pathway and is a target for cross-regulation of this pathway by the cAMP signaling system. The cAMP-activated protein kinase, PKA, inhibits Raf-1 by phosphorylation on S259. Here, we show that the cAMP-degrading phosphodiesterase-8A (PDE8A) associates with Raf-1 to protect it from inhibitory phosphorylation by PKA, thereby enhancing Raf-1's ability to stimulate ERK signaling. PDE8A binds to Raf-1 with high (picomolar) affinity. Mapping of the interaction domain on PDE8A using peptide array technology identified amino acids 454–465 as the main binding site, which could be disrupted by mutation. A cell-permeable peptide corresponding to this region disrupted the PDE8A/Raf-1 interaction in cells, thereby reducing ERK activation and the cellular response to EGF. Overexpression of a catalytically inactive PDE8A in cells displayed a dominant negative phenotype on ERK activation. These effects were recapitulated at the organism level in genetically modified (PDE8A$^{-/-}$) mice. Similarly, PDE8 deletion in *Drosophila melanogaster* reduced basal ERK activation and sensitized flies to stress-induced death. We propose that PDE8A is a physiological regulator of Raf-1 signaling in some cells.

V-raf-1 murine leukemia viral oncogene homolog 1 (Raf-1) is at the apex of the mitogen activated protein kinase (MEK)–ERK pathway, which controls many fundamental biological processes including cell proliferation, survival, and transformation. In this pathway Raf-1 phosphorylates and activates MEK, which in turn phosphorylates and activates ERK. ERK has more than 150 known substrates which mediate many of the pleiotropic functions of this pathway (1). Raf-1 regulation is complex and still is insufficiently understood. Critical events are the dephosphorylation of an inhibitory site, S259, which allows Raf-1 binding to activated rat sarcoma viral oncogene (Ras) and is a prerequisite for further activation (2, 3). S259 is a target for phosphorylation by PKA (4, 5) and is part of a complex system of crosstalk between the cAMP and the ERK pathways.

The cAMP system is the first signal-transduction system identified as mediating the intracellular biochemical effects of hormones (6), and PKA has been recognized as a main effector of cAMP (7). The intimate connections between the cAMP and ERK pathways were first revealed when PKA was shown to inhibit Raf-1 by direct phosphorylation (8–13). The exact mechanism of inhibition has remained unclear. Several phosphorylation sites in Raf-1 were invoked in the inhibitory action [e.g., S43, which could interfere with Raf-1 binding to Ras (13); S621, which can inhibit Raf-1 kinase activity directly (10); S233, which mediates inhibitory 14-3-3 binding; and S259, which blocks Raf-1 translocation to the plasma membrane and Ras binding (4, 5)]. Although the mechanistic function of most of these phosphorylation sites has remained controversial (14), S259 has emerged clearly as major inhibitory site whose dephosphorylation is part of the physiological activation process of Raf-1 and is mandatory for Raf-1 activation to ensue (2, 3). In addition, several other mechanisms of crosstalk have been discovered, including the regulation of Ras family proteins by cAMP-sensitive exchange factors and the phosphorylation of phosphodiesterases (PDEs) by ERK (15, 16).

Cyclic nucleotide PDEs terminate cAMP signaling by hydrolyzing cAMP, with this enzyme class featuring a large number of genes and isoforms that are regulated by differential expression, alternative splicing, and distinct modes of subcellular compartmentalization (17). Critically, studies on the cAMP-specific phoshodiesterase-4 (PDE4) family of enzymes have shown that the targeting of distinct PDE isoforms to specific signaling complexes and localities in cells underpins compartmentalized cAMP signaling (18, 19) and allows the development of spatially discrete gradients of cAMP that control spatially restricted subpopulations of the cAMP effectors PKA and exchange protein directly activated by cAMP (EPAC) (20).

Recently, there has been a surge of interest in the cAMP-specific phoshodiesterase-8 (PDE8) family of enzymes. PDE8s are expressed widely in human tissue (21) with functions in testosterone production (22), lymphocyte adhesion (23), chemotaxis (24), and excitation–contraction coupling in ventricular myocytes (25). PDE8 isoforms exhibit an extremely high affinity for cAMP (26), and this unique feature has led to the suggestion that PDE8 enzymes may have a very important cellular role in protecting any associated protein from fluctuations in basal cAMP concentrations. Compartmentalization of cAMP-specific PDEs with PKA substrates has been recognized as a mechanism that not only protects the substrates from inappropriate PKA

Significance

The ERK pathway is a ubiquitous mechanism for transducing a variety of extracellular signals into intracellular events. It also is misregulated in a number of different disease states including several cancers. The ERK pathway crosstalks with other signaling cascades, including the cAMP system. In this paper, we show that a key component of the ERK pathway, Raf-1 kinase, can associate with a specific cyclic nucleotide phosphodiesterase, phosphodiesterase 8A (PDE8A), to modulate the activity of the kinase. We report that the interaction between Raf-1 and PDE8A underpins functional consequences of ERK signaling in several different model systems.

Author contributions: K.M.B., B.Z., F.C., D.B.M., J.A.B., S.A.D., W.K., M.D.H., and G.S.B. designed research; K.M.B., J.P.D., E.H., K.H., F.C., D.R., S.T., L.C.Y.L., M.J.W., and M.S.-A. performed research; B.Z. and D.B.M. contributed new reagents/analytic tools; K.M.B., J.P.D., E.H., B.Z., K.H., F.C., D.R., S.T., L.C.Y.L., M.J.W., J.A.B., M.S.-A., S.A.D., W.K., M.D.H., and G.S.B. analyzed data; and J.A.B., W.K., M.D.H., and G.S.B. wrote the paper.

The authors declare no conflict of interest.

Freely available online through the PNAS open access option.

[1]To whom correspondence should be addressed. E-mail: beavo@u.washington.edu.

This article contains supporting information online at www.pnas.org/lookup/suppl/doi:10.1073/pnas.1303004110/-/DCSupplemental.

phosphorylation under basal conditions but also ensures specificity of action when a single receptor type is activated to produce a second messenger, such as cAMP, that is common to many other receptors (19). Here, we report that at least part of the PDE8A in the cell can bind tightly to Raf-1, regulate Raf-1 phosphorylation on S259, and, in so doing, regulate the cross-talk node whereby cAMP exerts an inhibitory effect on Raf-1 signaling, retarding subsequent ERK phosphorylation and activation.

Results

PDE8A Localizes with Raf-1 Immunoprecipitates. To look for binding partners for Raf-1, immunoprecipitates of Raf-1 from HEK293 cells were digested with trypsin and subjected to peptide map fingerprinting analysis using a mass spectrometer. PDE8A was identified as a 95-kDa Raf-1–associated protein with seven PDE8A peptides identified in the spectra (Fig. S1). To validate the interaction between Raf-1 and PDE8A, immunoprecipitates of Raf-1 were tested for PDE activity and were found to contain PDE activity that was inhibited by dipyridimole, an effective and partially selective PDE8 inhibitor (Fig. 1*A*). Because these data strongly suggested that PDE8A and Raf-1 can exist in a complex, Raf-1 immunoprecipitates were screened for associated PDE8A using Western blotting (Fig. 1*B*). With this technique, a PDE8A-specific antibody detected a protein of the correct weight that was associated with Raf-1. To verify further the association of Raf-1 and PDE8A, we undertook overexpression studies in which epitope-tagged constructs of Raf-1 (Myc tag) and PDE8A (Flag tag) were coexpressed in HEK293 cells, and immunoprecipitates of both tags were probed for both Myc–Raf-1 and Flag-PDE8A (Fig. 1*C*). Control immunoprecipitates used antibodies against an unrelated tag (vesicular stomatitis virus). Raf-1 coimmunoprecipitated with PDE8A, and vice versa. The PDE8A–Raf-1 association was not caused by nonspecific interaction, because the control immunoprecipitates showed no coimmunoprecipitating species. To determine whether the association of PDE8A and Raf-1 depended on cAMP concentrations within cells, the immunoprecipitations were repeated following treatment with forskolin alone or with forskolin in conjunction with either a nonspecific PDE inhibitor, 3-isobutyl-1-methylxanthine (IBMX), or a PDE8-selective inhibitor (Fig. 1 *D* and *E*). None of these treatments influenced the amount of PDE8A that copurified with Raf-1, or vice versa, suggesting that a preformed complex of PDE8 and Raf-1 exists in HEK293 cells.

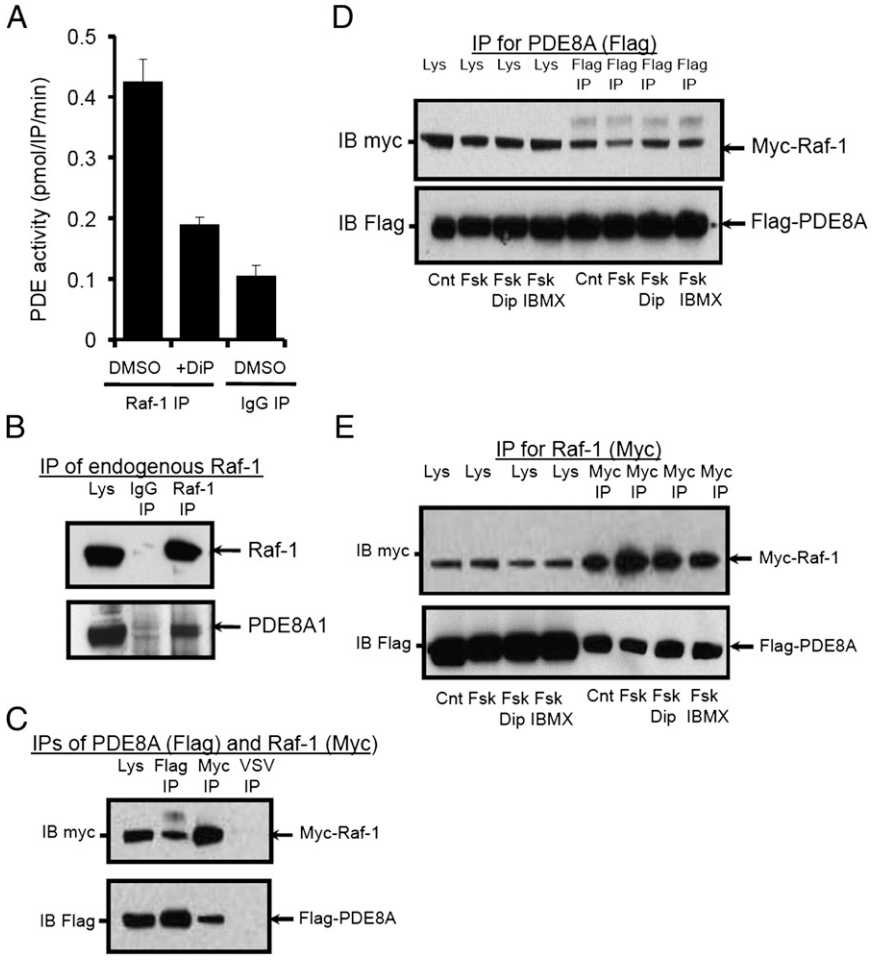

Fig. 1. PDE8 and Raf-1 form a constitutively assembled complex. (*A*) Immunoprecipitations (IP) of Raf-1 or control IgG from HeLa cells were analyzed for associated PDE activity. Raf-1 Immunoprecipitations contained PDE activity that was inhibited by 100 μM dipyridimole (DiP). (*B*) Immunoprecipitates of endogenous Raf-1 from HeLA cells brings down PDE8A1. (*C*) Tagged constructs of Raf-1 (Myc tag) and PDE8A (Flag tag) were coexpressed in HEK293, and immunoprecipitates of both tags were probed for both Myc-Raf-1 and Flag- PDE8A. IB, immunoblot. (*D* and *E*) Immunoprecipitates with PDE8A Flag antibody (*D*) and with Raf-1 Myc antibody (*E*). Immunoprecipitates as in *A* were repeated following treatment with forskolin alone (100 μM, 10 min) or with forskolin (100 μM, 10 min) in conjunction with either a nonselective PDE inhibitor (IBMX, 100 μM, 10-min pretreatment) or a PDE8-selective inhibitor (dipyridimole, 100 μM, 10-min pretreatment).

PDE8 Activity Regulates Raf-1 Phosphorylation at Ser259. Because the biochemical data presented above suggested an interaction between Raf-1 and PDE8A, we assessed whether PDE8 activity could influence the amount of basal phosphorylation of Raf-1 at S259 in HEK293 cells using Licor Odyssey technology, a quantitative Western blotting method (Fig. 2). PDE8A overexpression significantly reduced phosphorylation at S259. Conversely, expression of a catalytically inactive form of PDE8A (D/N-PDE8A) resulted in a dominant-negative phenotype, a concept we had developed previously in studies of PDE4 isoforms (27). Overexpression of this construct significantly augmented phosphorylation at S259 on Raf-1, presumably by displacing the endogenous PDE8A from its binding site on Raf-1 (Fig. 2). Treatment with the partially selective PDE8 inhibitor dipyridimole also significantly increased S259 phosphorylation of Raf-1. Additionally, increases in Raf-1 S259 phosphorylation that ensued upon treatment of cells with the adenylyl cyclase activator forskolin were either inhibited by PDE8A overexpression or augmented by D/N-PDE8A overexpression. Because PDE8A activity makes up a small percentage (<5%) of the total PDE activity in these cells but has such a profound effect on basal phospho-S259 Raf-1 levels (Fig. 2, bars 6, 7, and 8), but on not the global PKA phosphorylation of PKA substrates (Fig. S2), we decided to ascertain whether PDE8A and Raf-1 interact directly.

PDE8A Interacts Directly with Raf-1. To determine whether the interaction was direct, we incubated purified PDE8–myelin basic protein (MBP) with either GST–Raf-1 or GST alone and performed a GST-pulldown experiment (Fig. 3*A*). PDE8 copurified with GST–Raf-1 but not with GST alone, suggesting that the interaction between PDE8 and Raf-1 is direct. Finally, we determined the affinity of the interaction of PDE8A and Raf-1 via surface plasmon resonance (SPR) analysis (Fig. 3*B*). GST–Raf-1 was coupled to the chip using an anti-GST antibody (*Materials and Methods*) and was probed with MBP–PDE8A (Fig. 3*B*). The affinity of interaction was extremely high, being in the mid to low picomolar range (K_d <61 pM). However, because the affinity of the proteins was so high, less than 5% dissociation occurred during an extended assay time of 4 h, precluding an accurate determination of the rate of dissociation (Fig. 3*C*). Therefore, the upper limit of k_d has been used for calculating the equilibrium dissociation constant K_d. We additionally tested the effects of dipyridimole on the formation and stability of the complex, but this inhibitor did not alter the interaction between Raf-1 and PDE8A (Fig. 3*D*), indicating that inhibitor binding to the active site does not affect the interaction between PDE8 and Raf-1. Control chips that had reference surfaces consisting of immobilized GST alone showed no interaction with MBP–PDE8A.

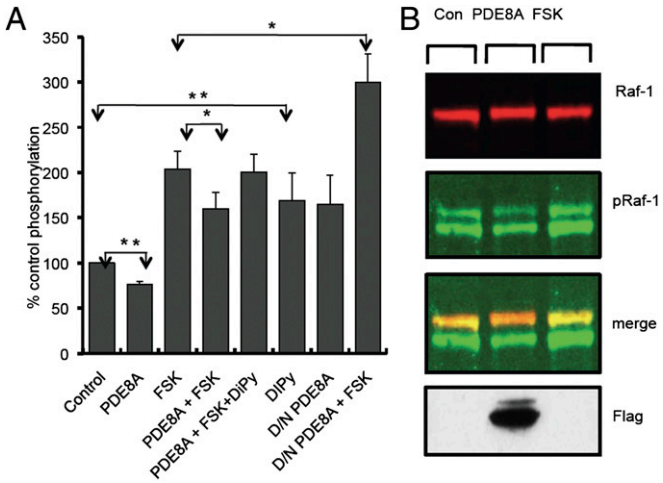

Fig. 2. PDE8 activity regulates phosphorylation of Raf-1 at serine 259. (*A*) HEK293 cells were transfected with Flag-PDE8A1 (lanes 2, 4, and 5) or dominant-negative PDE8A1 (lanes 7 and 8) and/or were treated with dipyridamole (DiP, lanes 5 and 6) or forskolin (FSK, lanes 3, 4, 5, and 8). The level of phospho-Raf-1 (S259) (pRaf-1) relative to total Raf-1 was monitored using a Licor Odyssey system, in which the band density measured using a pRaf-1 phospho-ser 259 antibody (*B*, second panel from the top) was divided by the total Raf-1 density (*B*, *Top*). The second panel from the bottom depicts the merged image of the upper two panels. Example data are from Licor Odyssey. (*Bottom*) Western blot showing relative expression of PDE8A construct. $n = 4$, with the exception of the dominant-negative PDE8A + forskolin sample, in which $n = 3$. *$P < 0.05$; **$P < 0.01$ relative to the control (Con) samples.

Mapping the Site of Interaction for Raf-1 on PDE8A. Peptide array technology has been successfully used by us (28–30) and others (31, 32) to map the interfaces between interacting proteins. This information can be used to design cell-permeable disrupting peptides and to inform mutagenesis strategies aimed at creating null-binding mutants (33, 34). To map the sites of interaction between Raf-1 and PDE8A, we synthesized a peptide array of human PDE8A consisting of 25mer peptides overlapping by five amino acids that encompassed the entire PDE8A sequence (Fig. 4). We then probed this array with either GST alone or GST–Raf-1 and detected areas of interaction by blotting for the GST tag. A robust interaction of GST–Raf-1 (but not GST alone) was identified on peptide spots 89, 90, and 91, which correspond to amino acids 442–476 within the PDE8A sequence (Fig. 4*A*). A detailed alanine scan of this region, in which successive residues were replaced by alanine residues, showed that the major residues involved in the interaction were D443, R454, R455, E460, Y461, and L463 (Fig. 4*B*). Further proof that the PDE8A sequence 454–461 (RRLSGNEY) was required for the association of Raf-1 was obtained using truncation analysis (Fig. 4*C*) of immobilized peptides. Stepwise C-terminal truncation revealed that this sequence was the minimum required to maintain Raf-1 binding.

To confirm the importance of PDE8A residues E460 and Y461 for the association of Raf-1, we mutated both residues to alanine and repeated the immunoprecipitation experiment from Fig. 1. Mutation of these residues attenuated but did not fully ablate the interaction of the proteins (Fig. 5*A*), suggesting that other residues in the 454–461 (RRLSGNEY) minimum binding region also were important for the formation of the Raf-1–PDE8A complex. Because a double alanine substitution of R454A:R455A was found to abolish Raf-1 interaction on peptide array (Fig. 4*B*), we combined this double mutation with the E460A:Y461A mutation. This quadruple mutant (R454A:R455:A:E460A:Y461A) further reduced binding to 15.3% ± 3.8% of the wild type (mean ± SE of $n = 3$; $P < 0.05$) (Fig. 5*B*), underlining the importance of this region in conferring interaction between PDE8A and Raf-1.

Peptide Disruption of the Raf-1–PDE8A Complex. Previous work from our laboratory has shown that cell-permeable analogs of 25mer peptides identified in this manner often can be used to disrupt signaling complexes within cells, thereby affecting specific functional outputs such as phosphorylation of the β2-adrenergic receptor by PKA (33) and the phosphorylation of β-arrestin by ERK MAPK (29). In this study, we used the Raf-1–docking sequence from PDE8A, encompassing residues R454–T465, to manufacture a stearylated, cell-permeable disruptor peptide. As a control, we also synthesized a scrambled version of the stearylated peptide that had the same net weight and charge (Peptide Cont). Both peptides had a C-terminal stearate group that allows transport across the cell membrane (29). The disruptor peptide, but not the control peptide, attenuated the association between PDE8A and Raf-1 when measured in immunoprecipitation experiments from cellular lysates (Fig. 5 *C* and *D*). The disruption of the complex induced by the peptide (33.8 ± 18.1%; $n = 3$, $P < 0.05$)

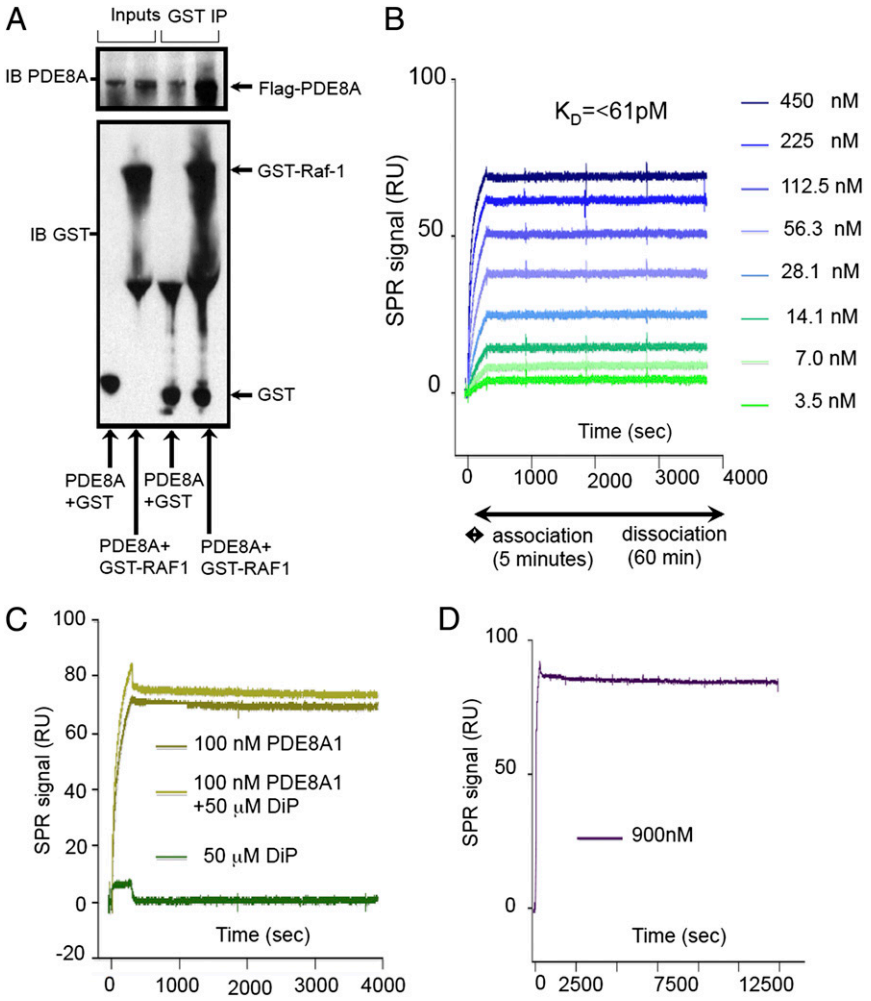

Fig. 3. PDE8A binds to Raf-1 with high affinity. (*A*) Purified PDE8–MBP was mixed with purified GST–Raf-1 or GST alone, and a GST-pulldown experiment was undertaken (*Materials and Methods*). (*B*) GST–Raf-1 was coupled to a Biacore chip using an anti-GST antibody and was probed with increasing concentrations of MBP–PDE8A. (*C*) MBP–PDE8A (100 nM) was used to probe a GST–Raf-1 chip. The injection was done with or without inclusion of 50 μM dipyridimole. A control injection of 50 μM dipyridimole was undertaken also. (*D*) Dissociation of the GST–Raf-1–PDE8–MBP complex was observed over 250 min.

was not as marked as that of the quadruple mutant R454A:R455:A:E460A:Y461A ($15.3 \pm 3.8\%$; $n = 3$, $P < 0.05$) (Fig. 5*B*), but this difference could be caused by cell permeability and affinity issues: Although we treated cells with a relatively high concentration of peptide (10 μM), we have no way of accurately measuring the amount that reaches the cell cytoplasm. We did, however, detect a 43% decrease in association of the endogenous proteins in HEK293 cells following treatment with disruptor peptide (Fig. S3*B*). It should be noted that, because the affinity of the interaction is extremely high (Fig. 3), we may not expect to achieve a complete disruption of a preformed complex between Raf-1 and PDE8A using a peptide. However, the disruptor peptide markedly decreased basal phospho-ERK in HEK293 cells (Fig. 6*A*) and increased basal phospho-Raf-1 levels (Fig. S3*A*) and could markedly attenuate phospho-ERK levels induced by short-term (0–3 min) EGF treatment (Fig. 6*B*).

In agreement with these results, overexpression of a catalytically inactive form of PDE8A exerted a dominant-negative action by significantly reducing resting phospho-ERK levels in HEK293 cells. In this case, however, the EGF-induced phospho-ERK response remained unaltered (Fig. 6*C*).

To determine whether the control of resting phospho-ERK levels by PDE8A activity occurs at the organismal level, we studied the phospho-ERK levels in wild-type fly strains that are known to exhibit canonical ERK signaling (35) and in a PDE8-knockout ($PDE8^{-/-}$) *Drosophila* mutant (Fig. 6*D*). We also determined phospho-ERK levels in the Leydig cells of an established PDE8A knockout ($PDE8A^{-/-}$) mouse model and compared them with the levels observed in matched wild-type controls (Fig. 6*E*). In agreement with the changes in basal phospho-ERK seen HEK293 cells, resting phospho-ERK levels were reduced markedly in both the PDE8-knockout fly and the PDE8A-knockout mouse. Phospho-ERK levels induced by 3-min EGF treatment also were reduced significantly in Leydig cells from PDE8A-knockout mice compared with the same cells isolated from wild-type mice (Fig. 6*E*).

Disruption of the PDE8A–Raf-1 Complex Alters Functional Responses to EGF and Stress Signals. Growth factor-induced morphological changes can be quantified in cells by measuring impedance (36, 37), which provides a real-time, noninvasive analysis suitable for measuring the kinetics of short- and long-term cellular responses. Changes in cellular impedance triggered by agents such as EGF and insulin have been shown to correlate with those measured by conventional means [e.g., autophosphorylation of the EGF receptor as measured by ELISA (36)], and impedance now is commonly used for assessing morphological changes such as membrane ruffling or formation of lamellipodia in a quantita-

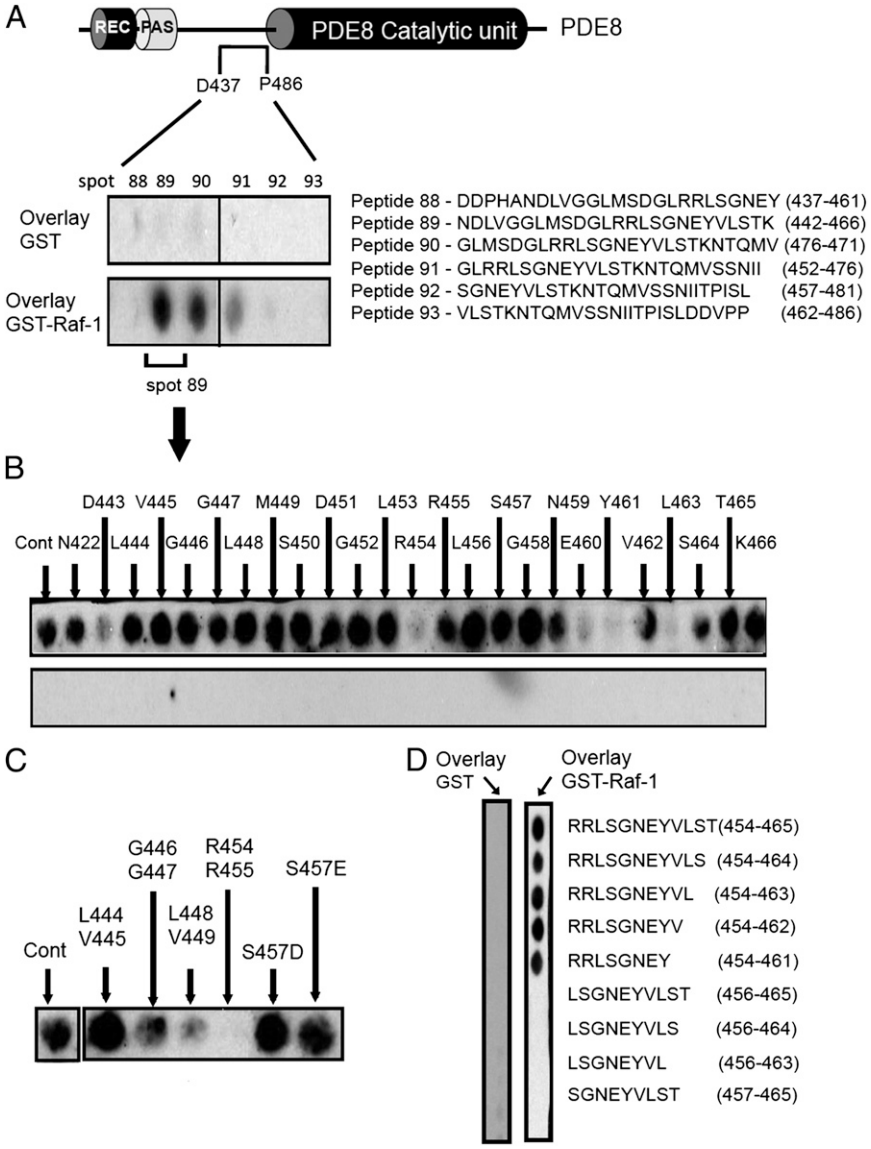

Fig. 4. Mapping of the Raf-1 binding site on PDE8A. (*A*) A peptide array of human PDE8A consisting of 25mer peptides overlapping by five amino acids that encompassed the entire PDE8A sequence was overlaid with either GST or GST–Raf-1. Positive interactions were detected with peptides 89, 90, and 91 that correspond to a sequence encompassing amino acids 442–476 of PDE8A1. (*B*) Peptide arrays in which successive residues (442–466) of the sequence within peptide 89 were replaced by alanine were overlaid with either GST or GST–Raf-1. (*C*) Stepwise C-terminal truncation of sequences within peptide 89 revealed the "core" binding motif that associates with Raf-1.

tive fashion. We used xCELLigence technology (Roche) to measure the impedance of cell cultures in which we perturbed the PDE8A–Raf-1 interaction.

First, to ensure a maximal signal, we constructed a dose–response curve in HeLa cells to evaluate the effect of increasing EGF concentration on cell impedance (the "cell index") (Fig. 7*A*). Maximal response occurred at 50 ng/mL EGF, a value reported previously by others as producing maximal impedance (36). Next we tested the effect of the disruptor peptide and control peptide on the maximal cell index produced in HeLa cells after EGF treatment (Fig. 7*B*). The disruptor peptide clearly attenuated the maximal increase in cell index, and this effect was mimicked by overexpression of the catalytically inactive (dominant-negative) PDE8A construct in HeLa cells (Fig. 7*C*). These data suggest that integrity of the PDE8A–Raf-1 complex is crucial for maximal EGF signaling leading to morphological changes. These results agree well with the premise that PDE8A activity is integral for the regulation of Raf-1–dependent ERK signaling in HEK293 cells, and primary mouse Leydig cells (Fig. 6).

Using impedance-based analysis, we also monitored the response of cells to stress, because loss of oxidative stress tolerance has been linked to the amplitude of the ERK signaling response (38). Treatment of HEK293 cells with either hydrogen peroxide or staurosporine reduced the cell viability to a level that was markedly enhanced by the transfection of a dominant-negative PDE8A construct (Fig. 7 *D* and *E*). Because hydrogen peroxide and staurosporine also can induce cell death, we assessed whether PDE8 plays a role in survival signaling. For this purpose we used *Drosophila melanogaster* as a model system. Indeed, we found that the disruption of the endogenous *PDE8* gene increased the sensitivity of flies to treatment with either hydrogen peroxide or paraquat. The survival rate of flies fed with 1% hydrogen peroxide was significantly reduced in male PDE8-

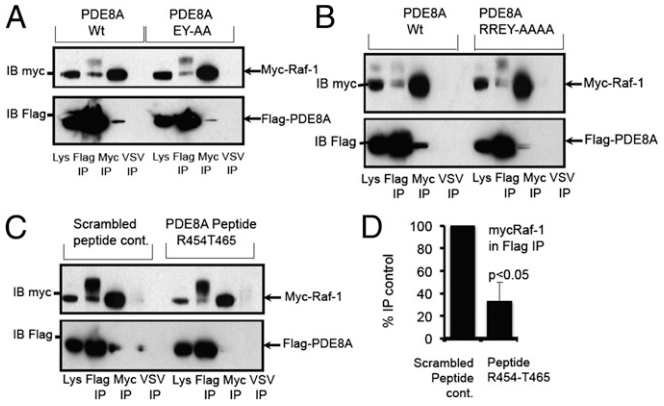

Fig. 5. Dissociation of the PDE8A–Raf-1 complex by site-directed mutagenesis and peptide disruption. (*A*) Mutation of PDE8A1 residues $^{460}E^{461}Y$ to alanines attenuated the interaction between PDE8A and Raf-1 as measured by coimmunoprecipitation. (*B*) Quadruple mutation of PDE8A1 residues $^{454}R^{455}R^{460}E^{461}Y$ to alanine further attenuated the interaction between PDE8A and Raf-1 as measured by coimmunoprecipitation. (*C*) A cell-permeable peptide corresponding to amino acids R454–T465 attenuated the association between PDE8A and Raf-1 when measured in immunoprecipitation experiments from cellular lysates. A randomly scrambled version of this peptide (Scrambled peptide control, cont.) did not affect the interaction between PDE8A and Raf-1. (*D*) Quantification of the effectiveness of the PDE8–Raf-1 disruptor peptide in dissociating the complex.

deficient flies as compared with the wild-type CantonS and Exilesis parents (Fig. 8*A*) and in female flies against both controls (Fig. 8*B*). The survival rate of male (Fig. 8*C*) and female (Fig. 8*D*) flies fed with 20 mM paraquat was significantly reduced in PDE8-deficient flies compared with both control strains. Thus, PDE8 function enhances survival at both the cellular and the organism levels.

Discussion

Regulation of Raf activity is of pivotal important to the control of cell growth, survival, and differentiation through the ERK signaling pathway (1). One important point of control is the inhibitory phosphorylation of Raf-1 by PKA. However, to date the factors that influence this key regulatory event have been obscure. Here we identify a means of controlling this inhibitory process through sequestration of the cAMP-hydrolyzing PDE8A enzyme with Raf-1 itself. The importance of individual PDE families is becoming more appreciated, especially in the light of the bewildering complexity of PDE isoform expression and the often very specific biological effects of isoform-selective PDE inhibitors (18). The cAMP effector PKA also can bind to Raf-1, but, in contrast to PDE8A, the binding of PKA to Raf-1 is disrupted by cAMP agonists (4). Thus, PDE8A may function as a local, tonic antagonist of cAMP signaling, setting the threshold that needs to be overcome for Raf-1 activation. This view is consistent with our results, because we show that displacement of endogenous PDE8A by a catalytically inactive species generates a dominant-negative phenotype (Figs. 2 and 7). Additionally, the effects of a cell-permeable PDE8A disruptor peptide and genetic silencing of PDE8A to reduce the basal local PDE8A activity and subsequent increase in Raf-1 activation (Fig. 6) also add weight to this proposal.

This identification of only the second binding partner identified for PDE8A [PDE8A also associates with IκB (39)] and of a PDE associated with Raf-1 strongly suggests that spatial regulation of Raf-1 can occur through sequestration of PDE8A. This finding may open opportunities to manipulate Raf-1 activation by pharmacological agents that modulate PDE8A and to evaluate changes in this system in disease states. Raf-1 activation is increasingly in the limelight as a promising drug target. Although Raf-1 is rarely mutated in cancer (40), B-Raf frequently is mutated in melanoma (41), and the B-Raf–selective inhibitor PLX4720 has shown impressive clinical efficacy in the treatment of B-Raf–mutated melanomas (42). However, in melanomas with Ras mutations, these inhibitors were ineffective and even may cause tumor progression. The reason seems to be a paradoxical activation of ERK caused by the promotion of Raf-1–B-Raf heterodimerization, which is stimulated by mutant Ras and Raf inhibitors (43, 44). The B-Raf–Raf-1 heterodimer has kinase activity>30-fold higher than that of the respective homodimers or monomers, even when one of the two Raf kinases is inactivated (45). Thus, despite being pharmacologically inhibited, B-Raf can recruit Raf-1 for signaling and efficient activation of the ERK pathway. In this context, PDE8A inhibitors should be beneficial and possibly synergistic with Raf inhibitors; as is shown here, PDE8A inhibition can impede the activation of Raf-1. This hypothesis is supported by recent findings that melanocytes use B-Raf to activate ERK, because Raf-1 activity is suppressed by high cAMP levels (46). However, in response to Ras mutations occurring during melanoma development, cells switch to use Raf-1 to activate the ERK pathway (46). This switch is promoted by mutant Ras stimulating a negative-feedback phosphorylation of B-Raf by ERK and an elevation of PDE4 activity. This shift deinhibits Raf-1 and enables Raf-1–mediated oncogenic signaling. In fact, inhibiting Raf-1 by activating cAMP signaling blocks proliferation and induces apoptosis of Ras-mutated melanoma cells (47). Thus, PDE8A-selective inhibitors may become important pharmacological agents to counteract oncogenic Raf signaling.

Materials and Methods

Cell Culture and Transfection. HEK 293 and HeLa cells were cultured in DMEM supplemented with 10% FCS, 1% penicillin-streptomycin, and 1% L-glutamine (all from Sigma) at 37 °C in humidified air with 5% CO_2 [all concentrations are (vol/vol)]. Transfections were performed using Polyfect (Qiagen) according to the manufacturer's instructions. Primary mouse Leydig cells were prepared and cultured from wild-type and PDE8A$^{-/-}$ mice as previously described (22). All animal usage and procedures were approved by the Institutional Animal Care and Use Committee of the University of Washington in accordance with the National Institutes of Health.

Mammalian Cell-Expression Constructs. Human Flag-tagged PDE8A1 in the pCMV-2 plasmid was a gift from Kenji Omori (Tanabe Seiyaku Co. Ltd., Japan). The pEF-myc-Raf-1 construct was provided by Chris Marshall (Institute of Cancer Research, London), and pGEX-KG-Raf-1 was described previously (10). For single transfections, 8 μg of DNA was used per 100-mm plate; for dual transfections, 4 μg of each construct was transfected.

Chemicals and Antibodies. Forskolin, dipyridamole, and IBMX (Sigma) were dissolved in DMSO and were added to cell media at a concentration of <0.1% DMSO. EGF, staurosporine, and hydrogen peroxide were all obtained from Sigma. Antibodies against the myc tag (1:2,000), phospho-ERK (1:1,000), ERK (1:1,000), and phospho-Raf-1 (pS259; 1:1,000) were obtained from Cell Signaling. Raf-1 (1:2,000) and PDE8A (1:2,000) antibodies were purchased from BD Biosciences and Scottish Biomedical, respectively. HRP-conjugated Flag antibody (1:2,000) was from Sigma, and GST antibody (1:2,000) was obtained from Santa Cruz.

PDE Assay and Cellular Transfection of PDE8A1. PDE activity was measured using a radioactive cAMP hydrolysis assay that has been described previously (27). [8-^{3}H] Adenosine cyclic-3′, 5′-monophosphate was from Amersham Biosciences, and cyclic-3′, 5′-monophosphate was obtained from Sigma. The substrate concentration used for PDE assays was 150 nM. Raf-1 immunoprecipitations were done from 400 μg of cellular lysate.

MS Analysis of Raf-1 Immunoprecipitates. Growing cells (1×10^7) were lysed in PBS supplemented with 1% Triton X-100 and protease inhibitors (Complete protease inhibitor mixture tablets; Roche) and phosphatase inhibitors (PhosSTOP tablets; Roche). Lysates were cleared by centrifugation (20,000 × *g* for 10 min), and the supernatant was immunoprecipitated with Raf-1

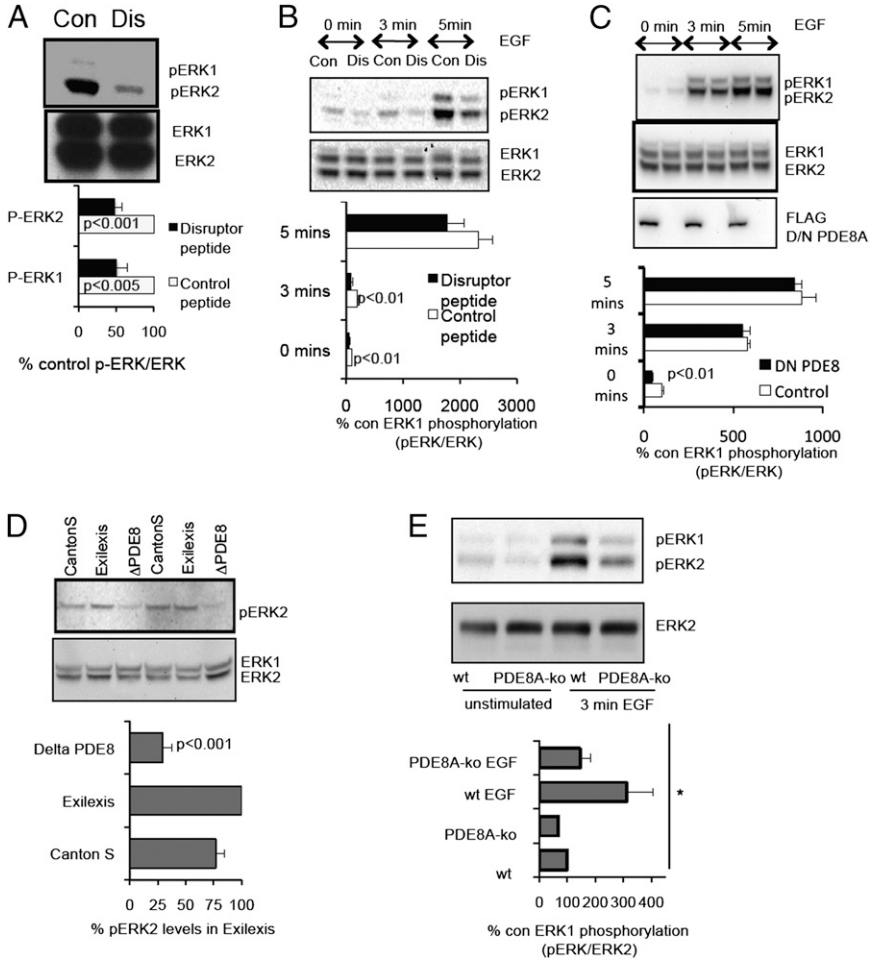

Fig. 6. Manipulation of the PDE8–Raf-1 complex alters the strength of basal and EGF-stimulated phospho-ERK signals. (*A*) Treatment of HEK293 cells with the disruptor peptide (Dis) significantly down-regulated basal phospho-ERK Map kinase levels compared with cells treated with the scrambled peptide control (Con). $n = 3$. (*B*) Pretreatment of HEK293 cells with disruptor peptide, but not scrambled control, significantly attenuated phospho-ERK levels induced by short-term (0- to 3-min) EGF treatment. (*C*) Overexpression of D/N PDE8 significantly reduced resting phospho-ERK levels in HEK293 cells. (*D*) Basal phospho-ERK levels are decreased significantly in the PDE8 knockout *Drosophila* compared with two control lines. (*E*) Basal phospho-ERK levels, and those induced by short-term (0- to 3-min) EGF treatment are attenuated in primary mouse Leydig cells derived from the PDE8A$^{-/-}$ mouse as compared with those derived from a wild-type mouse. $n = 3$. *$P = 0.037$, one-way ANOVA.

antibodies for 2 h at 4 °C. Immunoprecipitates were washed three times in lysis buffer and separated on 7.5% SDS gels. Gels were stained with colloidal Coomassie stain (0.1% Coomassie R-250, 50% methanol, 5% acetic acid, and 45% Milli-Q water) and were destained in destaining solution (40% methanol, 10% acetic acid, and 50% Milli-Q water) until the background was clear. Bands were cut out from the gel and chopped into ~1-mm^2 pieces. The gel pieces were washed with distilled water for 15 min, followed by two washes with 100 mM NH_4HCO_3/CH_3CN (50:50 vol/vol) for 15 min. Then gel pieces were crushed with a Teflon pestle, dehydrated in CH_3CN, and dried in a SpeedVac (Thermo Fisher Scientific) for 5 min. Gel pieces were incubated with 12.5 mg/mL of modified porcine trypsin (Promega) in 20 mM NH_4HCO_3/0.1% nOctyl-Glucoside at 30 °C overnight. Then an equal volume of CH_3CN was added to the digest, followed by incubation at 30 °C for 30 min on a shaking platform. The digest supernatant was removed and dried down in a SpeedVac. The digest was resuspended in 10 mL of 50% CH_3CN in 0.1% trifluoric acid and was analyzed on a Voyager-DE Pro MALDI-TOF (Applied Biosystems) by peptide mass fingerprinting using 2,5-dihydroxy benzoic acid as matrix.

Western Blotting. Cells were lysed in 3T3 lysis buffer [1% Triton X-100, 50 mM Hepes (pH 7.2), 10 mM EDTA, and 100 mM $NaH_2PO_4{\cdot}2H_2O$] supplemented with a protease inhibitors tablet (Roche). Detergent-insoluble proteins were removed by centrifugation at 10,000 × *g* for 10 min. Aliquots of the soluble fraction were resolved by SDS/PAGE using the NuPAGE system (Invitrogen). Proteins were transferred to nitrocellulose membrane (Protran; Whatman GmbH) for 1 h at 25V using NuPAGE Transfer buffer. The membranes were blocked in 5% nonfat dry milk (Marvel, Premier International Foods)/Tris-buffered saline supplemented with 0.1% Tween-20 (TBS-T) for at least 1 h before primary antibodies were added in 1% Marvel/TBS-T and incubated at 4 °C overnight. The membranes were washed three times for 10 min in TBS-T. Peroxidase- or Alexa Fluor-conjugated secondary antibodies were added in 1% Marvel/TBST and incubated for 1 h at room temperature. Membranes were washed as before, and bound primary antibodies were detected by incubation with appropriate secondary antibodies using either ECL or the Licor Odyssey scanner for fluorescence detection. Densitometry on film was performed using Quantity One software (BioRad Laboratories). Fluorescence intensity was measured using the Odyssey software (Licor). For ECL detection, the mouse (Amersham) and rabbit (Sigma) secondary antibodies were used at a 1:5,000 concentration. The Odyssey secondary antibodies Alexa-Fluor 680 and Alexa-Fluor 800 were diluted 1:10,000.

Immunoprecipitation Experiments. Myc-Raf-1 and Flag-PDE8A1 were immunoprecipitated from 400 –1,000 μg of total protein lysate made up to a total volume of 400 μL with 3T3 lysis buffer using 50 μL Myc (Sigma) or Flag (Invitrogen) antibodies coupled to agarose beads. The immunoprecipitates were incubated for at least 2 h or overnight at 4 °C with constant agitation before the beads were washed at least three times with 3T3 lysis buffer. For endogenous immunoprecipitates, 10 μg PDE8A antibody was incubated with 1,000 μg HeLa cell lysate overnight at 4 °C with constant agitation. Washed protein-G beads (Amersham) (75 uL) were added for 1–2 h before the beads were pelleted and washed as above.

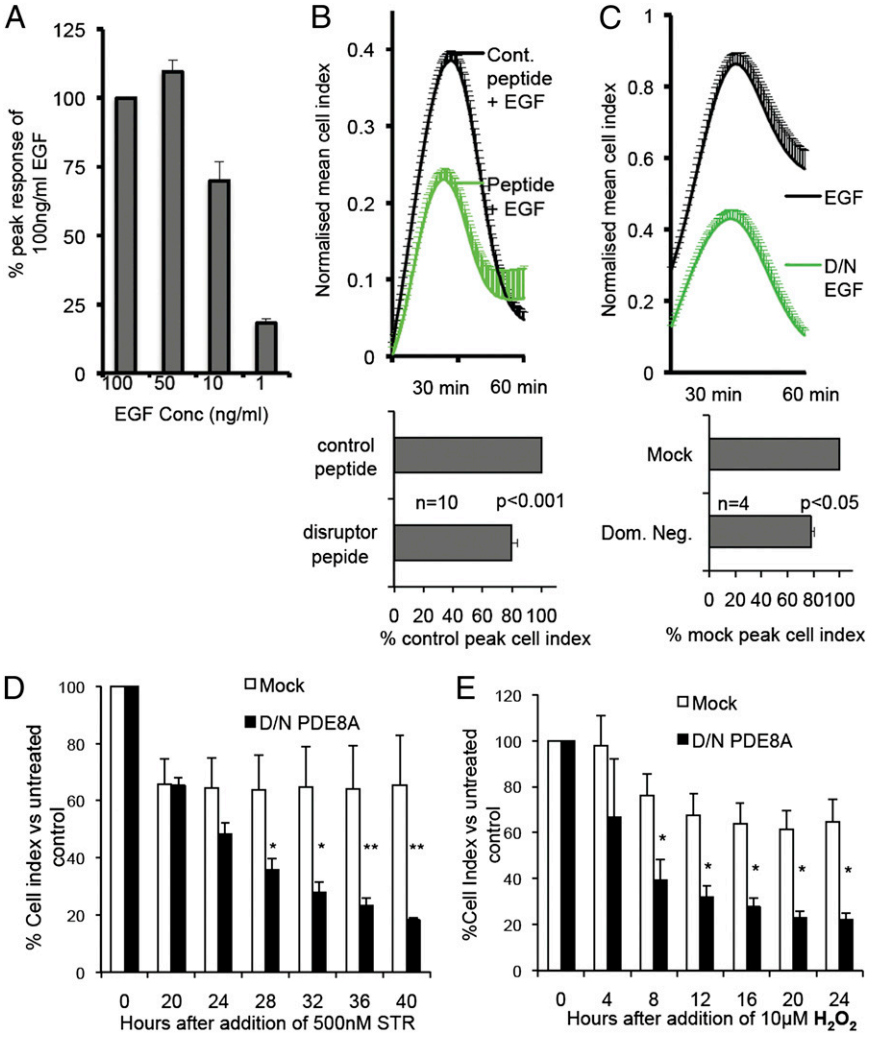

Fig. 7. Disruption of the PDE8–Raf-1 complex alters functional responses to EGF and stress signals. (*A*) The EGF-induced change of cell shape in HeLa cells measured by real-time impedance measurement is dose dependent. (*B*) The PDE8–Raf-1 disruptor peptide but not the scrambled control (cont) attenuates the cell-shape change induced by EGF in HeLa cells. (*C*) Overexpression of D/N PDE8A significantly reduced cell-shape changes in HeLa cells induced by EGF. (*D*) Cell death induced in HEK293 cells by treatment with 500 nM staurosporine is enhanced when cells are transfected with D/N PDE8A. (*E*) Cell death induced in HEK293 cells by treatment with 10 μM hydrogen peroxide is enhanced when cells are transfected with D/N PDE8. $*P < 0.05$, $**P < 0.01$.

Peptide Arrays. Peptide libraries were produced by automatic SPOT synthesis (48). They were synthesized on continuous cellulose membrane supports on Whatman 50 cellulose membranes using 9-fluorenylmethyloxycarbonyl chemistry with the AutoSpot-Robot ASS 222 (Intavis Bioanalytical Instruments). The interactions of spotted peptides with GST and GST–Raf-1 were determined by overlaying the membranes with 10 μg/mL recombinant protein. Bound proteins were detected with GST antibody (Santa Cruz), and detection was performed with a secondary anti-rabbit antibody coupled with HRP (1:2,500 dilution; Dianova) and ECL detection.

Disruptor Peptides. All peptides were purchased from GenScript and dissolved in DMSO. The disruptor peptide (R454–T465) RRLSGNEYVLST was designed based on the results of the peptide array. The scrambled control peptide SYTVRLLGERNS sequence was created by randomly scrambling the disruptor peptide sequence, ensuring no vital residues were in the same position. To make them cell permeable, peptides were synthesized with a stearic acid group [$CH_3(CH_2)_{16}COOH$] attached to the C terminus. Peptides were added to cells at a final concentration of 10 μM for 4 h before cells were harvested.

Site-Directed Mutagenesis. Site-directed mutagenesis was performed using the QuickChange kit (Stratagene). All primers were obtained from Thermo Scientific, and sequencing was performed by the DNA Sequencing Service at the University of Dundee, Dundee, Scotland. The following primers were used to create the required mutations:

R454A/R455A mutant:

Forward primer: 5′-CTTAATGTCTGATGGTTTGGCGGCCCTATCAGGGAATGAATATGTTC-3′

Reverse primer: 5′-GAACATATTCATTCCCTGATAGGGCCGCCAAACCATCAGACATTAAG-3′

E460A/Y461A mutant:

Forward primer: 5′-CTATCAGGGGAATGCAGCTGTTCTTTCAACAAAAAACACTCAAATGG-3′

Reverse primer: 5′-CCATTTGAGTGTTTTTTGTTGAAAGAACAGCTGCATTCCCTGATAG-3′

Both R454A/R455A and E461A/Y461A mutants were verified by sequencing using the F3 primer (*SPR Experiments*).

R454A/R455A/E460A/Y461A mutants:

Forward primer: 5′-gggcttaatgtctgatggtttggcagcactatcagggaatgcagctgtt-3′

Reverse primer: 5′-aacagctgcattccctgatagtgctgccaaaccatcagacattaagccc-3′

PDE8A1 dominant negative D726A mutant:

Forward primer:; 5′-gctgattaaatgtgctgctgtgtccaatccctgcc-3′

Reverse primer: 5′-ggcagggattggacacagcagcacatttaatcagc-3′

The D726A mutant was verified by sequencing using the CMV24 primer 5′-GTGCCCACCAGCCTTGTCCTAATA-3′.

HEK293 cells overexpressing wild-type Flag-PDE8A1, D/N PDE8A1 and mock transfected cells were blotted for immunoreactivity and normalized to equal expression levels. The catalytic activity of D/N PDE8A1 versus wild-type PDE8A1 was measured by PDE assay as described elsewhere (27).

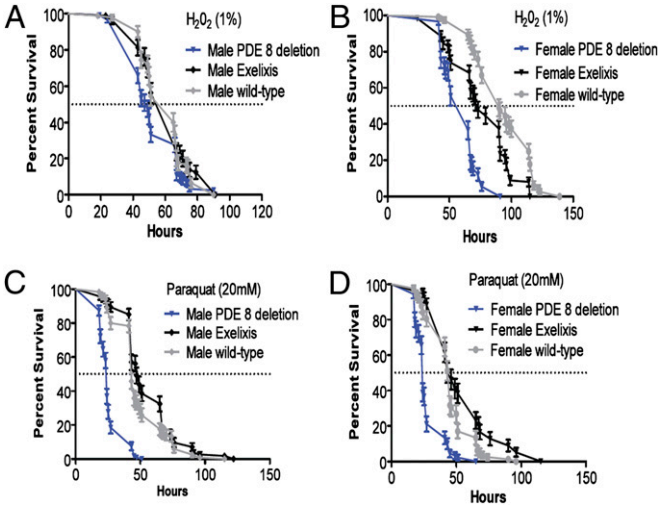

Fig. 8. Silencing of PDE8 alters survival responses to oxidative stress in *Drosophila*. (*A* and *B*) The survival rate of flies fed with 1% hydrogen peroxide is reduced significantly in (*A*) male PDE8-deficient flies as compared with the wild-type CantonS ($P = 0.0138$) and Exilesis ($P < 0.0001$) parents (log-rank Mantel–Cox test) and in (*B*) female PDE8-deficient flies ($P < 0.0001$ against both controls). (*C* and *D*) The survival rate of (*C*) male and (*D*) female flies fed with 20 mM paraquat is significantly reduced in PDE8-deficient flies as compared with both control strains ($P < 0.0001$; log-rank; Mantel–Cox test).

In Vitro Binding Assay. Equimolar amounts (2 μM) of purified recombinant GST (negative control) and GST–Raf-1 and PDE8A1 protein (Scottish Biomedical) were mixed in binding buffer [50 mM Tris·HCl (pH7.5), 100 mM NaCl, 2m M $MgCl_2$, 1 mM DTT, 0.5% (vol/vol) Triton X-100, 0.5% (wt/vol) BSA, and protease inhibitors] and were incubated for 1 h at 4 °C. Then 30 μL of GST beads were washed and equilibrated in binding buffer, added to the protein mixture, and incubated as before for 1 h. Beads were sedimented by centrifugation at 10,000 × *g* for 1 min, and washed three times. Proteins associated with the beads were eluted by boiling in sample buffer and were analyzed by Western blotting.

SPR Experiments. SPR analysis was performed using a Biacore 2000 instrument (GE Healthcare). Anti-GST antibody (GST Capture Kit, GE Healthcare) was immobilized to a level of 15,000 response units (RU) onto CM5 sensor chips (GE Healthcare) according to the manufacturer's instructions. The fusion protein GST–Raf-1 (100 nM) was reversibly captured to a level of 165–200 RU. As control surface, an anti-GST surface captured with GST (1 μg/mL) was prepared. The interaction study was performed in HBS buffer [20 mM Hepes (pH 7.4), 150 mM NaCl, and 0.01% surfactant Tween20] at 30 °C. Kinetic constants were determined by injecting a series of dilutions of MBP–PDE8A1 (900–3.5 nM) over GST–Raf-1 on the capture surfaces at a flow rate of 30 μL/min. The association was monitored for 5 min, and dissociation of the complex was followed for 60 min. Because less than 5% of the complex dissociates within 60 min, the dissociation time of the highest concentration (900 nM) was prolonged to 480 min and used for quantification of the dissociation rate constant (k_d). After each interaction event, the antibody surface was regenerated using two pulses of 10 mM glycine (pH 1.7). Data were evaluated using the software BIAevaluation 4.1 (GE Healthcare) and Graphpad Prism 5.04 (GraphPad Software Inc.). Kinetic rate constants (k_a and k_d) were determined by simultaneously fitting experimental data to rate equations derived from a Langmuir 1:1 binding model. Because the k_d can be determined accurately only if at least 5% of bound material dissociates, the upper limit of k_d has been calculated using the equation $k_d = -\ln(0.95)/td$, where td is the time (in seconds) allowed for dissociation. Sensorgrams were double referenced using the control surface (GST) and blank buffer injections to subtract baseline drifts from the data sets. To assess reproducibility of kinetic constants, the analysis was performed in duplicate.

To test whether the interaction between PDE8A1 and Raf-1 is inhibited by a selective PDE8 inhibitor, MBP–PDE8A1 (100 nM) was preincubated with 50 μM dipyridimole and injected over GST–Raf-1 on the capture surfaces. The binding mode of dipyridimole and GST Raf-1 was tested separately in a control experiment.

To generate the MBP–PDE8A1 bacterial expression vector, the Flag–PDE8A1 construct was used as a template to amplify the PDE8A1 insert and incorporate the *SalI* and *XbaI* recognition sites by PCR using the following primers:

Forward primer: 5′-AATCTAGAATGGGCTGTGCCCCGA-3′

Reverse primer: 5′-AAGTCGACCTATTCAGGAGGTGGTC-3′

The PCR product and pMAL–c2x vector (New England BioLabs) were digested using *XbaI* and *SalI* restriction enzymes and ligated. The construct was sequenced using the following primers:

Forward 1 primer: 5′-GATGAAGCCCTGAAAGACGCGCAG-3′

Reverse 1 primer: 5′-GAT TTA ATC TGT ATC AGG-3′

Forward 2 primer: 5′-GAA GAG TTG TCC GTA ATG-3′

Reverse 2 primer: 5′-GCA GGG ATT GGA CAC ATC-3′

Forward 3 primer: 5′-ATA TCC GAA TGT GTT CAG-3′

Reverse 3 primer: 5′-CAC ATC AGC AGA ATG TGT-3′

To purify Raf-1 and PDE8A1 proteins for the SPR experiments, a 10-mL overnight culture of BL21 *Escherichia coli* cells containing the pGEX–GST–Raf-1 or pMAL–c2x plasmids was added to 500 mL of LB medium and grown at 37 °C with shaking until the OD_{600} reached ∼0.6. Expression of the recombinant fusion proteins was induced by adding 0.1 mM isopropyl-β-D-1-thiogalactopyranoside. After 4 h cells were pelleted by centrifugation at 7,000 × *g* for 7 min and were frozen at −80 °C to assist with lysis. The bacterial pellet was lysed as described (49), and fusion proteins were isolated by incubating the lysates with either glutathione Sepharose beads or amylose resin (Amersham) for 1 h at 4 °C. Beads were washed six to eight times in PBS, and the fusion proteins were released by incubating with 600 μL of elution buffer [10 mM glutathione in 50 mM Tris (pH 7.5) or 50 mM maltose] for 20 min at 4 °C. The elution step was repeated three times, and the eluates were pooled. Any detergent, glutathione, or maltose was removed by overnight dialysis using the Slide-A-Lyzer cassettes (Piercenet) in 2 L of dialysis buffer.

Measuring Cellular Responses with the xCELLigence System. To measure cellular responses with the xCELLigence system, the RTCA SP instrument (Roche Applied Science) was used according to the supplier's instructions. The E-plate 96 (Roche), a single-use, disposable, 96-well microtiter plate with gold cell-sensor arrays in the bottom that allow the impedance inside each well to be monitored and assayed in real time, was used to perform cell-based assays as previously described by G.S.B. (28). The impedance is reported as arbitrary cell index measurements. HeLa cells were transfected with D/N PDE8A and 24 h later were seeded onto a 96-well E-plate (Roche) at a density of 2×10^4 cells per well. Cells were allowed to adhere overnight before any treatment. For disruptor peptide experiments, cells were treated with the peptides for 4 h before further treatment. Then, cells were serum starved for 4 h before treatment with 100 ng/mL EGF. After treatment, the cell index was measured every 15 s using the xCELLigence system (Roche). To measure cell death after treatment with 500 nM staurosporine or 10 μM hydrogen peroxide, HEK293 cells were plated as described above, and the cell index was measured every 30 min. Cell viability was measured by calculating the cell index of treated cells as a percentage of nontreated cells.

Generation of the PDE8 Deletion in *Drosophila*. The *Drosophila* PDE8 deletion was generated using flippase recombinase and two lines containing flippase recognition target-bearing *piggybac* insertions. The *piggybac* insertions lines ($PDE8^{d06642}$ and $PDE8^{f02577}$) flank most of the PDE8 coding region including the entire catalytic domain. Individual lines were screened with PCR of genomic DNA to confirm the loss of the intervening DNA.

***Drosophila* Survival Assays in Response to Oxidative Stress.** Flies of specified genotype (5-d-old males and females, housed separately) were starved for 4 h and then exposed to 20 mM paraquat or 1% H_2O_2 (both from Sigma) in 1% sucrose medium in groups of 30, with three biological replicates. Flies were counted until 100% mortality was reached, and data were expressed as percent survival ± SEM ($n = 3$). Data were assessed for significance by the log-rank (Mantel–Cox) test using GraphPadPrism 5.0 software.

Whole-Fly Phospho-ERK Western Blot Analysis. Basal phospho-ERK levels were analyzed from PDE8-deficient flies compared with two control strains, wild-type CantonS flies and Exilexis flies, to control for the genetic background of PDE8-deficient line. Briefly, 50 flies of each genotype were washed and gently homogenized in ice-cold 3T3 lysis buffer supplemented with 1:100 dilution of protease-inhibitor mixture (Sigma) using an Eppendorf micropestle. The homogenate then was subjected to two successive centrifugations at 1,000 × *g* at 4 °C for 5 min to remove large cuticle debris and wings, and the protein concentration was determined using the Bio-Rad Bradford assay.

ACKNOWLEDGMENTS. K.M.B., J.P.D., F.C., M.D.H., and G.S.B. were supported by Grants G0600765 from the Medical Research Council (UK) and 06CVD02 from the Fondation Leducq. This work also was supported by the Science Foundation Ireland under Grant 06/CE/B1129 (to D.R. and W.K.); by the European Union Sixth Framework Programme Specific Targeted Project thera-cAMP (Contract 037189); by the Seventh Framework Programme Collaborative Project AffinityProteome (Contract 222635) (B.Z. and K.H.); by National Institutes of Health Grants NS29740 (to D.B.M.) and GM083926 (to J.A.B.); and by the Biotechnological and Biological Sciences Research Council (UK) Grant BB/G020620/1 (to S.A.D).

1. Yoon S, Seger R (2006) The extracellular signal-regulated kinase: Multiple substrates regulate diverse cellular functions. *Growth Factors* 24(1):21–44.
2. Kubicek M, et al. (2002) Dephosphorylation of Ser-259 regulates Raf-1 membrane association. *J Biol Chem* 277(10):7913–7919.
3. Jaumot M, Hancock JF (2001) Protein phosphatases 1 and 2A promote Raf-1 activation by regulating 14-3-3 interactions. *Oncogene* 20(30):3949–3958.
4. Dumaz N, Marais R (2003) Protein kinase A blocks Raf-1 activity by stimulating 14-3-3 binding and blocking Raf-1 interaction with Ras. *J Biol Chem* 278(32):29819–29823.
5. Dhillon AS, et al. (2002) Cyclic AMP-dependent kinase regulates Raf-1 kinase mainly by phosphorylation of serine 259. *Mol Cell Biol* 22(10):3237–3246.
6. Sutherland EW, Robison GA (1966) The role of cyclic-3′,5′-AMP in responses to catecholamines and other hormones. *Pharmacol Rev* 18(1):145–161.
7. Walsh DA, et al. (1972) Cyclic AMP-dependent protein kinases from skeletal muscle and liver. *Adv Cyclic Nucleotide Res* 1:33–45.
8. Cook SJ, McCormick F (1993) Inhibition by cAMP of Ras-dependent activation of Raf. *Science* 262(5136):1069–1072.
9. Burgering BM, Pronk GJ, van Weeren PC, Chardin P, Bos JL (1993) cAMP antagonizes p21ras-directed activation of extracellular signal-regulated kinase 2 and phosphorylation of mSos nucleotide exchange factor. *EMBO J* 12(11):4211–4220.
10. Häfner S, et al. (1994) Mechanism of inhibition of Raf-1 by protein kinase A. *Mol Cell Biol* 14(10):6696–6703.
11. Sevetson BR, Kong X, Lawrence JC, Jr. (1993) Increasing cAMP attenuates activation of mitogen-activated protein kinase. *Proc Natl Acad Sci USA* 90(21):10305–10309.
12. Graves LM, et al. (1993) Protein kinase A antagonizes platelet-derived growth factor-induced signaling by mitogen-activated protein kinase in human arterial smooth muscle cells. *Proc Natl Acad Sci USA* 90(21):10300–10304.
13. Wu J, et al. (1993) Inhibition of the EGF-activated MAP kinase signaling pathway by adenosine 3′,5′-monophosphate. *Science* 262(5136):1065–1069.
14. Matallanas D, et al. (2011) Raf family kinases: Old dogs have learned new tricks. *Genes Cancer* 2(3):232–260.
15. Gerits N, Kostenko S, Shiryaev A, Johannessen M, Moens U (2008) Relations between the mitogen-activated protein kinase and the cAMP-dependent protein kinase pathways: Comradeship and hostility. *Cell Signal* 20(9):1592–1607.
16. Houslay MD, Kolch W (2000) Cell-type specific integration of cross-talk between extracellular signal-regulated kinase and cAMP signaling. *Mol Pharmacol* 58(4): 659–668.
17. Conti M, Beavo J (2007) Biochemistry and physiology of cyclic nucleotide phosphodiesterases: Essential components in cyclic nucleotide signaling. *Annu Rev Biochem* 76:481–511.
18. Houslay MD (2010) Underpinning compartmentalised cAMP signalling through targeted cAMP breakdown. *Trends Biochem Sci* 35(2):91–100.
19. Baillie GS (2009) Compartmentalized signalling: Spatial regulation of cAMP by the action of compartmentalized phosphodiesterases. *FEBS J* 276(7):1790–1799.
20. Zaccolo M (2011) Spatial control of cAMP signalling in health and disease. *Curr Opin Pharmacol* 11(6):649–655.
21. Wang H, et al. (2008) Kinetic and structural studies of phosphodiesterase-8A and implication on the inhibitor selectivity. *Biochemistry* 47(48):12760–12768.
22. Vasta V, Shimizu-Albergine M, Beavo JA (2006) Modulation of Leydig cell function by cyclic nucleotide phosphodiesterase 8A. *Proc Natl Acad Sci USA* 103(52):19925–19930.
23. Vang AG, et al. (2010) PDE8 regulates rapid Teff cell adhesion and proliferation independent of ICER. *PLoS ONE* 5(8):e12011.
24. Dong H, Osmanova V, Epstein PM, Brocke S (2006) Phosphodiesterase 8 (PDE8) regulates chemotaxis of activated lymphocytes. *Biochem Biophys Res Commun* 345(2): 713–719.
25. Patrucco E, Albergine MS, Santana LF, Beavo JA (2010) Phosphodiesterase 8A (PDE8A) regulates excitation-contraction coupling in ventricular myocytes. *J Mol Cell Cardiol* 49(2):330–333.
26. Soderling SH, Bayuga SJ, Beavo JA (1998) Cloning and characterization of a cAMP-specific cyclic nucleotide phosphodiesterase. *Proc Natl Acad Sci USA* 95(15):8991–8996.
27. McCahill A, et al. (2005) In resting COS1 cells a dominant negative approach shows that specific, anchored PDE4 cAMP phosphodiesterase isoforms gate the activation, by basal cyclic AMP production, of AKAP-tethered protein kinase A type II located in the centrosomal region. *Cell Signal* 17(9):1158–1173.
28. Baillie GS, et al. (2007) Mapping binding sites for the PDE4D5 cAMP-specific phosphodiesterase to the N- and C-domains of beta-arrestin using spot-immobilized peptide arrays. *Biochem J* 404(1):71–80.
29. Meng D, et al. (2009) MEK1 binds directly to betaarrestin1, influencing both its phosphorylation by ERK and the timing of its isoprenaline-stimulated internalization. *J Biol Chem* 284(17):11425–11435.
30. Anthony DF, et al. (2011) β-Arrestin 1 inhibits the GTPase-activating protein function of ARHGAP21, promoting activation of RhoA following angiotensin II type 1A receptor stimulation. *Mol Cell Biol* 31(5):1066–1075.
31. Bjørgo E, et al. (2010) Cross talk between phosphatidylinositol 3-kinase and cyclic AMP (cAMP)-protein kinase a signaling pathways at the level of a protein kinase B/beta-arrestin/cAMP phosphodiesterase 4 complex. *Mol Cell Biol* 30(7):1660–1672.
32. Perino A, et al. (2011) Integrating cardiac PIP3 and cAMP signaling through a PKA anchoring function of p110γ. *Mol Cell* 42(1):84–95.
33. Smith KJ, et al. (2007) 1H NMR structural and functional characterisation of a cAMP-specific phosphodiesterase-4D5 (PDE4D5) N-terminal region peptide that disrupts PDE4D5 interaction with the signalling scaffold proteins, beta-arrestin and RACK1. *Cell Signal* 19(12):2612–2624.
34. Rampersad SN, et al. (2010) Cyclic AMP phosphodiesterase 4D (PDE4D) Tethers EPAC1 in a vascular endothelial cadherin (VE-Cad)-based signaling complex and controls cAMP-mediated vascular permeability. *J Biol Chem* 285(44):33614–33622.
35. Friedman AA, et al. (2011) Proteomic and functional genomic landscape of receptor tyrosine kinase and ras to extracellular signal-regulated kinase signaling. *Sci Signal* 4(196):rs10.
36. Atienza JM, et al. (2006) Dynamic and label-free cell-based assays using the real-time cell electronic sensing system. *Assay Drug Dev Technol* 4(5):597–607.
37. Staršíchová A, et al. (2009) Dynamic Monitoring of Cellular Remodeling Induced by the Transforming Growth Factor-β1. *Biol Proced Online* 11:316–324.
38. Ikeyama S, Kokkonen G, Shack S, Wang XT, Holbrook NJ (2002) Loss in oxidative stress tolerance with aging linked to reduced extracellular signal-regulated kinase and Akt kinase activities. *FASEB J* 16(1):114–116.
39. Wu P, Wang P (2004) Per-Arnt-Sim domain-dependent association of cAMP-phosphodiesterase 8A1 with IkappaB proteins. *Proc Natl Acad Sci USA* 101(51): 17634–17639.
40. Zebisch A, Troppmair J (2006) Back to the roots: The remarkable RAF oncogene story. *Cell Mol Life Sci* 63(11):1314–1330.
41. Davies H, et al. (2002) Mutations of the BRAF gene in human cancer. *Nature* 417(6892):949–954.
42. Flaherty KT, et al. (2010) Inhibition of mutated, activated BRAF in metastatic melanoma. *N Engl J Med* 363(9):809–819.
43. Poulikakos PI, Zhang C, Bollag G, Shokat KM, Rosen N (2010) RAF inhibitors transactivate RAF dimers and ERK signalling in cells with wild-type BRAF. *Nature* 464(7287):427–430.
44. Heidorn SJ, et al. (2010) Kinase-dead BRAF and oncogenic RAS cooperate to drive tumor progression through CRAF. *Cell* 140(2):209–221.
45. Rushworth LK, Hindley AD, O'Neill E, Kolch W (2006) Regulation and role of Raf-1/B-Raf heterodimerization. *Mol Cell Biol* 26(6):2262–2272.
46. Dumaz N, et al. (2006) In melanoma, RAS mutations are accompanied by switching signaling from BRAF to CRAF and disrupted cyclic AMP signaling. *Cancer Res* 66(19): 9483–9491.
47. Marquette A, André J, Bagot M, Bensussan A, Dumaz N (2011) ERK and PDE4 cooperate to induce RAF isoform switching in melanoma. *Nat Struct Mol Biol* 18(5): 584–591.
48. Kramer A, Schneider-Mergener J (1998) Synthesis and screening of peptide libraries on continuous cellulose membrane supports. *Methods in Molecular Biology*; Combinatorial peptide library protocols *Methods Mol Biol* 87:25–39.
49. Frangioni JV, Neel BG (1993) Solubilization and purification of enzymatically active glutathione S-transferase (pGEX) fusion proteins. *Anal Biochem* 210(1):179–187.